Arab J Sci Eng (2014) 39:547–555
DOI 10.1007/s13369-013-0821-9

RESEARCH ARTICLE - PHYSICS

Analytical Model of Multi-junction Solar Cell

Muhammad Babar · Arslan A. Rizvi · Essam A. Al-Ammar · Nazar H. Malik

Received: 1 September 2012 / Accepted: 31 January 2013 / Published online: 9 November 2013

Abstract Multi-junction solar cells (MJSCs) are a current trend in the field of solar cells and form the backbone of concentrated photovoltaic systems. They are an attractive option because of their high efficiency, better power production and cost effectiveness. The aim of this paper is to present a general mathematical model of MJSC, suitable for computer simulation. This model investigates cell characterization curves including current density and power curves as a function of voltage for different concentration levels and number of junctions. The effect of varying material properties of junctions and tunneling layers is also analyzed. Two different types of MJSCs have been tested on the model, including InGaP–GaAs dual-junction solar cell with tunneling layer of InGaP and InGaP–GaAs–Ge triple-junction solar cell with tunneling layers of GaAs. Paper also presents the simulation results which are in agreement with practical conclusions.

Keywords Concentrated photovoltaic · Modeling simulation · Multi-junction solar cell · Tunnel junction

M. Babar (✉) · E. A. Al-Ammar · N. H. Malik
Department of Electrical Engineering, King Saud University, Riyadh 11421, Saudi Arabia
e-mail: engr.mbabar@gmail.com; mbabar@ksu.edu.sa

M. Babar
Institute of Industrial and Manufacturing Engineering, PNEC, National University of Science and Technology, Karachi, Pakistan

A. A. Rizvi
Sustainable Energy Technologies, King Saud University, Riyadh 11421, Saudi Arabia
e-mail: aarizvi4@hotmail.com

الخلاصة

تُعد الخلايا الشمسية المتعددة (MJSC) هي الاتجاه الحالي في مجال الخلايا الشمسية، وتشكل العمود الفقري للشمسية الضوئية المركزة (CPV). فهي تشكل خيارا جذابا بسبب كفاءتها العالية، وتحسن الفعالية الإنتاجية من حيث التكلفة. إن الهدف من هذه الورقة هو تقديم نموذج رياضي عام للخلايا الشمسية المتعددة بحيث تكون مناسبة للمحاكاة الحاسوبية. وتحقق في هذا النموذج توصيف الخلايا في المنحنيات بما في ذلك كثافة التيار ومنحنيات الطاقة، وكذلك تحليل تأثير تغيير خصائص المواد في التقاطعات الرياضية وطبقات الشرائح الشمسية. وقد تم اختبار نوعين مختلفين من الخلايا الشمسية المتعددة على النموذج، بما في ذلك الخلية الشمسية ثنائية وثلاثية الوصلة للغاليوم InGaP-GaAs. وتقدم الورقة أيضا نتائج المحاكاة التي تتفق والاستنتاجات العملية.

1 Introduction

Recent research in the new generation of solar cells has led to use of large solar spectrum for better efficiency. Multi-junction solar cell (MJSC) is a combination of different types of photovoltaic junctions stacked over one another via homo-junctions, intrinsic materials or tunnel junctions. Different solar cells having different bandgap energies and physical properties are combined to efficiently capture and convert a large range of photon wavelengths into useful electrical power. Presently, MJSCs are capable of generating approximately twice as much power as the conventional solar cell of the same area [1–6].

The studies show that much higher efficiencies can be achieved by increasing the number of solar cell layers [1]. This involves concept of concentrated photovoltaic (CPV) in which light is concentrated over the panel via reflectors. The solar concentration level is usually divided into four regions. As the concentration level increases, Multi-junction does not only face tracking and thermal management issues, but also the resultant increase in current densities also influences the stability of the tunnel junction [7–11].

Multi-junction solar cells have a higher theoretical conversion efficiency as compared to other photovoltaic technologies [12]. Recently, solar cell has beaten its previous record of efficiency, i.e., 40.7 % ,which was achieved with a MJSC by Boeing Spectrolab Inc. in December 2006 [13] and now Solar Junction (San Jose, California, US) has announced a new world-record conversion efficiency of 44 % for a production-ready solar photovoltaic (PV) cell using its multi-junction technology [14]. The individual subcells of a multi-junction cell are interconnected via Esaki interband tunnel diodes [15,16]. They feature both low electrical resistivity and high optical transmissivity. These are the key issues for connecting the cells monolithically [15,17,18]. In [19], Guter experimentally investigated and characterized tunnel diodes used in monolithic III–V MJSCs and in [20], Hermle discussed in detail the effect of tunneling current in MJSCs. In [21], Jung reported fabrication of InGaP tunnel diode in tandem cells. In [22], Takamoto performed microscopic analysis of GaInP/GaAs tandem cell and reported its efficiency with GaInP tunnel Junction. In [23], Ahmed reported improved structure of GaAs tunnel junction which allows it to work on higher temperatures as well. There are many publications concerning the microscopic electrical to molecular level modeling and experimental viewpoints on MJSC.

A large number of models are required for observing the performance characteristics of MJSC. Moreover, all models are not compatible with each other. This makes the selection quite hard and perplexing. The paper proposes an alternative strategy and methodology for modeling to determine performance characteristics of MJSC for different environmental conditions. Firstly, this paper discusses fundamental features of MJSC. Then, the MJSC design and performance are presented and the comparison between the different tunnel layers is discussed. Paper further discusses in detail the physical model of MJSC and implements the proposed model in Simulink/MATLAB. Finally, the paper concludes with simulation results of MJSCs.

2 Multi-Junction Solar Cell Structure

Consider the MJSC of triple-junction structure shown in Fig. 1. The triple-junction consists of a GaInP solar cell as the top layer, GaAs in the middle, and Ge layer as bottom layer. The double junction consist of InGaP as top cell and GaAs as bottom cell. Moreover, these are joined together with a special junction called tunnel junction and are also provided with window layers. Window layers prevent surface recombination and smooth out the lattice change by introducing a gradient between the materials. The band gap of this material is selected such that it is higher than that of the cells below it. Thus, window junction solves the problem of lattice mismatch, but that of connecting different cells with one another

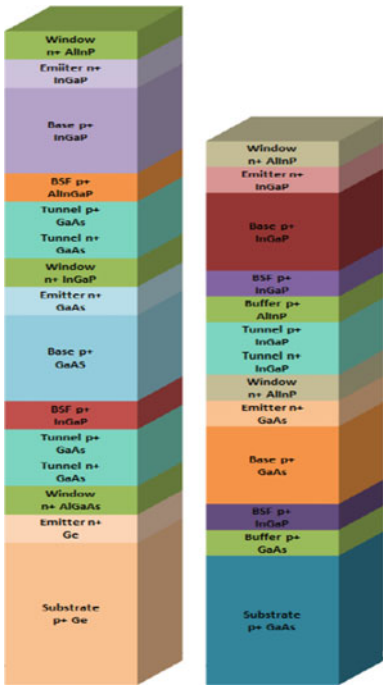

Fig. 1 *Right* Dual-junction solar cell prototype structure, *Left* Triple-junction solar cell prototype structure [4,6,13]

is solved by creating a tunnel junction instead of a normal junction.

The tunnel junction allows bi-directional current flow. Since, each cell acts as a current source and all cells are connected in series in a MJSC, therefore the resultant current is limited by the smallest current source. Since, top cells are expected to absorb more photons and thus leaving less photons for the next cell in line, the last cell might produce the least current and limit the overall current output. Hence, a compromise between the thickness and shadowing must be achieved to ensure optimal power production in a MJSC.

3 Comparison Between Tunnel Layers

Usually, the multi-junction PV cells contain tunnel junctions of AlInAs/GaInP, InGaP/GaAs, GaAs/GaAs and GaInP/GaInP. The two structures which are discussed here contain tunnel junction of GaAs/GaAs and GaInP/GaInP with window and buffer layer of AlGaAs. The ideal I–V characteristic, peak voltage and current, specific resistivity and doping concentration for these junctions are given in Table 1.The specific resistivity is calculated from the I–V characteristics for the junction and is defined as [21–24].

$$\rho_c = \left(\frac{\partial V}{\partial J}\right) \tag{1}$$

where ∂V is the voltage applied and ∂J is the current density [24,25].

Table 1 Parametric values of tunnel junctions

	Peak voltage (mV)	Peak current (mA)	I_p/I_v ratio	Specific resistivity	Doping concentration ($/cm^3$)	Bandgap (eV) @300K
Ge/Ge	105	37	6/1	0.17×10^{-3}	8e−18/1e−19	0.67
GaAs/GaAs	195	35	12/1	7.8×10^{-3}	8e−18/1e−19	1.42
GaInP/GaInP	140	40	9/7	1.0×10^{-3}	8e−18/1e−19	1.9

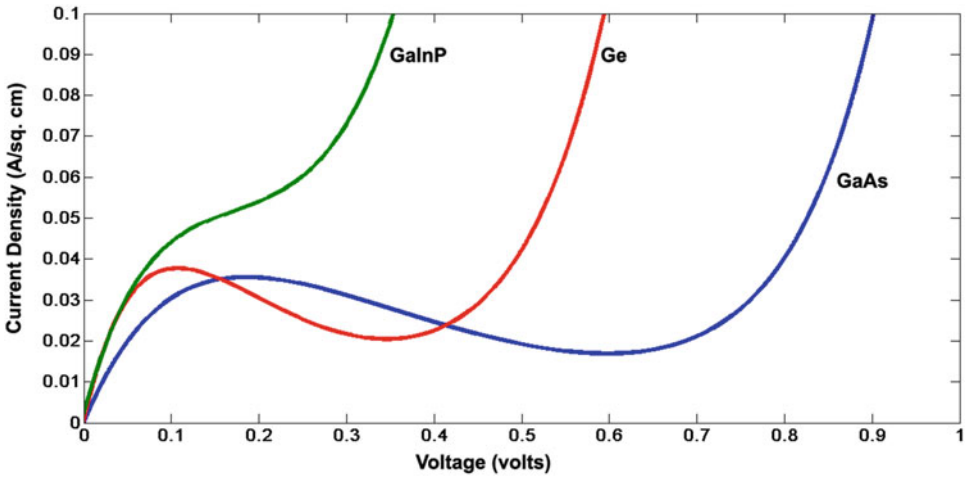

Fig. 2 I–V curve of Ge–Ge, GaAs–GaAs and GaInAs–GaInAs tunnel junctions

The I–V characteristics by generalized tunnel junction model for both junctions are shown in Fig. 2. The non-linear nature of junction is apparent since the output current of a cell depends on the cell's terminal operating voltage and temperature. It has been found that the three region of GaAs/GaAs and Ge/Ge junction are evidently vivid; one region exhibits negative resistance and other has positive resistance. However, in GaInP/GaInP junction, negative resistance region does not exist. Since, the carrier flow is faster in GaInP rather than GaAs, different tunnel junctions are considered for combining different cells for producing MJSC to have proper lattice and current matching.

4 Physical Model

The physical structure of the MJSC could easily be generalized as a solar cell connection in series with tunnel diode.

4.1 Solar Cell Model

The mathematical model of current/voltage characteristics for a PV cell has been discussed in literature [26–29]. The general photovoltaic cell model consists of a parallel-connected photocurrent source, a diode, a resistor representing a leakage current, and a series resistor to account for internal resistance to the current flow. Moreover, the voltage–current characteristics of a solar cell can be expressed as [30,31]:

$$J = J_{\mathrm{L}} - J_0 \left\{ \mathrm{e}^{\left[\frac{q(V+J_{r_s})}{n\mathrm{KT}}\right]} - 1 \right\} - \frac{V + J_{r_s}}{r_{\mathrm{SH}}} \tag{2}$$

where; J = current density (A/cm^2), J_{L} = photogenerated current density (A/cm^2), J_0 = reverse saturation current density (A/cm^2), J_{r_s} = specific series resistance ($\Omega\mathrm{cm}^2$) and r_{SH} = specific shunt resistance ($\Omega\mathrm{cm}^2$).

4.2 Tunnel Junction Model

Tunneling in a MJSC refers to the phenomenon of the fast movement of carriers across the potential barrier. Tunneling is a significant aspect of charge transport in MJSCs. Tunneling layer provides low resistive and efficient functionality. In a conventional junction, conduction takes place while the junction is forward biased whereas, a forward-biased tunnel junction gives rise to three functional regions where an increase in forward voltage is accompanied by a decrease in the forward current. Theoretically, all three regions of tunnel junction are described by exponential functions. Because of this peculiar I–V characteristic, tunnel junction has a significance effect on the MJSC behavior. The general I–V characteristics of tunnel diode is shown in Fig. 2. These characteristics can be expressed as [16]:

$$J_{\mathrm{TOTAL}} = \frac{V(t)}{V_p} J_T + J_X + J_{TH} \tag{3}$$

where;

$$J_T = J_p e^{1-\frac{V(t)}{V_p}}$$
$$J_X = J_v e^{A_2(V(t)-V_v)}$$
$$J_{TH} = J_s e^{\frac{qV(t)}{kT}-1}$$

Here, J_{TOTAL} = total current density of the tunnel diode, J_T = closed-form expression of the tunneling current density which describes the behavior particular to the tunnel diode, J_{X} = the excess tunneling current density, J_{TH} = normal diode characteristic equation, J_p = peak current density, V_p = peak voltage, J_v = valley current density, V_v = valley voltage, A_2 = excess current prefactor, J_s = saturation current density, q = charge of an electron, k = Boltzmann's constant and T = temperature in degree Kelvin.

It should be noted that J_p and V_p are strongly influenced by the doping concentration and doping profile of the material. The forward voltage of this device is the same as that of a diode. Thus,

$$V_{\mathrm{F}} = \frac{\mathrm{kT}}{q} ln \frac{(N_{\mathrm{A}} N_{\mathrm{D}})}{n_i^2} \tag{4}$$

where; V_{F} = forward voltage, N_{A} = acceptor concentration, N_{D} = donor concentration, n_i = intrinsic carrier concentration [31,32].

The valley current depends on the peak current density of the tunnel layer. Normally, the ratio of GaAs peak current density and valley current density is $\frac{1}{12}$, while the Ge tunneling layer has a ratio of $\frac{1}{6}$ and GaInP tunneling layer has a ratio of $\frac{7}{9}$. Moreover, the junction capacitance of tunnel junction can be expressed as [16]:

$$C_j = \begin{cases} \frac{C_{T_0}}{\left(1-\frac{V_j}{\phi}\right)^{\Gamma}} & \text{if } -V_j > 0 \\ \frac{C_{T_0}+V_j\left(C_{T_0}V_j+\frac{C_{T_0}}{\phi}\right)}{1+e^{10\left(V_j-0.8\phi\right)}} & \\ +\frac{C_{T_0}}{\Gamma^{0.2}\left(e^{10\left(0.8\phi-V_j\right)}-1\right)} & \text{if } -V_j < 0 \end{cases} \tag{5}$$

where; V_j = voltage across tunnel junction, C_{T_0} = zero bias depletion capacitance, Γ = built-in barrier potential and ϕ = capacitance power law parameter.

5 Multi-Junction Model

The solar cell in proposed model is the collective representation of all photovoltaic junctions having short-circuit current as its series-matched current as discussed earlier. Furthermore, the collective model also incorporates series and parallel resistances, whereas the open-circuit voltage is the sum of the junction voltages.

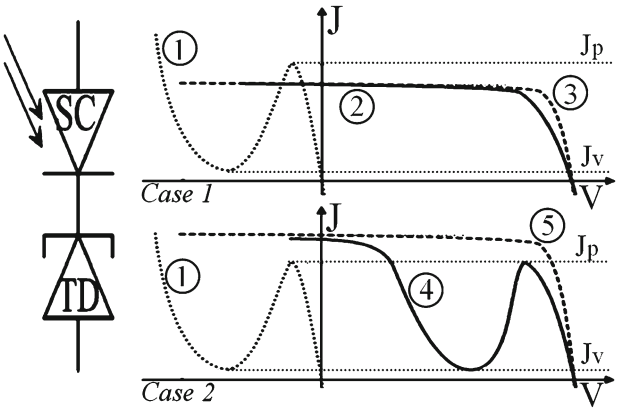

Fig. 3 Effect of tunneling layer in solar cell [20,27–29]

The tunnel diode, because of a highly non-linear relationship between its current density and applied voltage, causes an undesirable situation when it is modeled in series with the MJSC model. Therefore, two different cases should be considered so as to understand the tunneling effect.

Case 1: if the overall photon-generated current density J is less than the peak current density of the tunnel junction J_p, then the cell tunneling would only have a very small ohmic resistance and can be modeled as a wire connection between the two cells of a MJSC.

Case 2: if the irradiation is increased and J crosses the peak current density of the tunnel junction J_p, then three modes of the tunnel junction are available and a dip appears in the current density. Figure 3 shows the two discussed cases at different levels of solar concentration; curve 1 shows the I–V curve of tunnel diode, curves 3 and 5 show I–V curves at different solar irradiations, and curves 2 and 4 illustrate the resulting I–V curves [19,20,33].

In 2006, Guter and Bett presented the practical study of hysteric behavior in MJSCs and other tunnel diode structures [9]. They also discussed the theoretical reasoning for hysteric behavior observed in tunnel diodes and similar devices. In Reference [19], authors calculated the theoretical current voltage (I–V) characteristics of tunnel diodes and solar cells when measured via four-wire techniques and compared with experimentally measured I–V curves using a similar model. This proposed model takes care of hysteric behavior in MJSCs by incorporating the numerical model of tunnel junction. To check the efficacy and applicability of the proposed analytical model, simulation model has been developed on Simulink/MATLAB.

6 Simulation Model

The simulation model of the tunneling layer of a MJSC has been derived from its physical model as discussed in Sect. 4. The model is used to simulate and investigate the performance characteristics of the tunneling layer. This model can

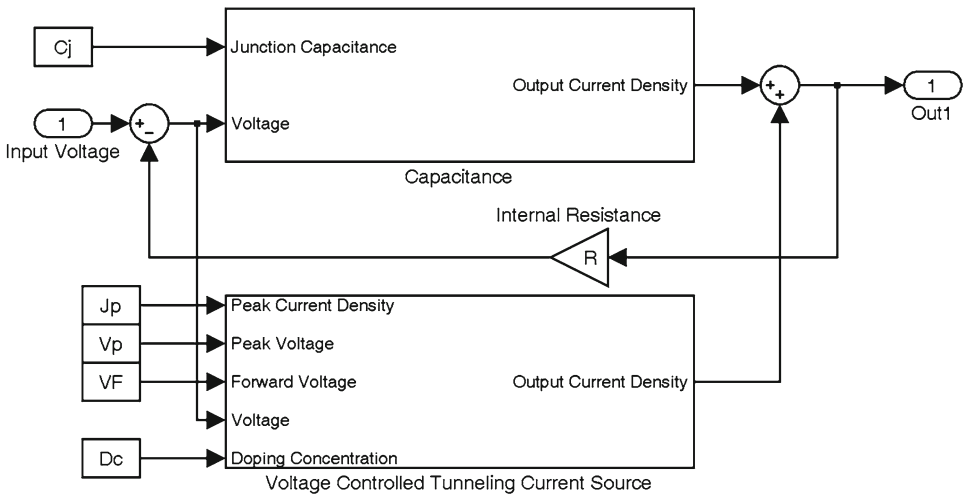

Fig. 4 Block diagram of the tunnel junction

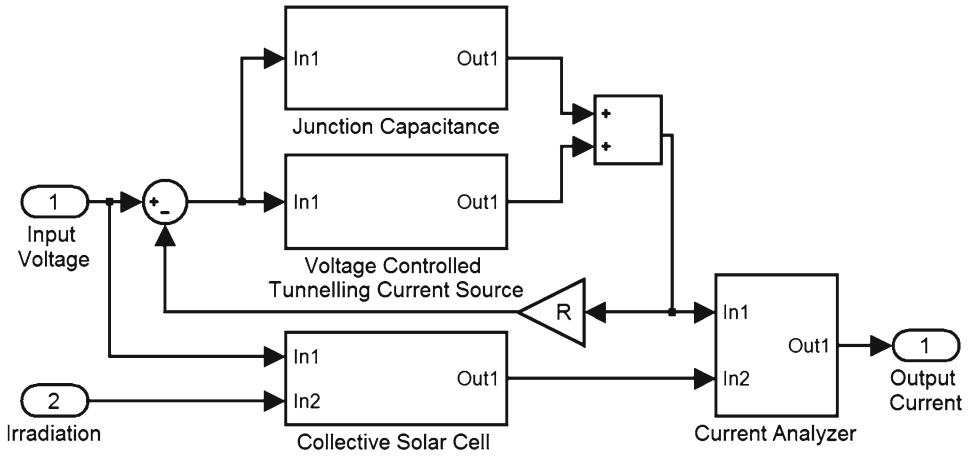

Fig. 5 MATLAB simulation block diagram

also be used to simulate the effect of doping concentration, peak current density and peak voltage of the tunneling layer of a MJSC. Figure 4 shows the block diagram of the model developed in Simulink/MATLAB. Where, capacitance block in Fig. 4 represents the junction capacitance of the tunneling layer. This block essentially executes the realistic behavior of the tunnel layer and determines its current density in all three working regions. The model uses the peak current density (J_P), respective peak voltage (V_P), forward voltage (V_F), doping concentration (D_c), internal resistance (R) and junction capacitance (C_j) as the input parameters.

It is important to build a generalized model suitable for all of the MJSCs which can be used to design and analyze performance characteristics of different materials. A generalized MJSC model is built using Matlab/Simulink to illustrate its I–V and P–V characteristics under different levels of irradiation. The proposed model is shown in Fig. 5.

7 Simulation Results

For the simulation of tunnel layer model, (GaAs) and (Ge) layers are considered. Table 2 shows realistic values for peak current density, respective peak voltage, junction capacitance, respective doping concentration and forward voltage of the tunnel layer for the mentioned materials [24,25,34].

Table 2 Parametric values of Ge and GaAs tunnel junctions at different doping concentrations [20,35,36]

Material	J_p (mA)	V_p (mV)	V_F (mV)	C_j (pF)	D_c (/cm$_3$)
Ge	5	70	480	3	2.14×10^{17}
	10	80	500	8	3.15×10^{17}
	20	90	540	20	6.80×10^{17}
	50	100	565	50	1.10×10^{18}
	100	110	575	100	1.33×10^{18}
GaAs	5	135	1,050	3	1.23×10^{15}
	10	115	1,100	8	3.23×10^{15}
	20	175	1,125	20	5.22×10^{15}
	50	195	1,150	50	8.45×10^{15}
	100	205	1,175	100	1.37×10^{16}

Figure 6 shows the current density versus voltage curves for different values of doping concentration as described in

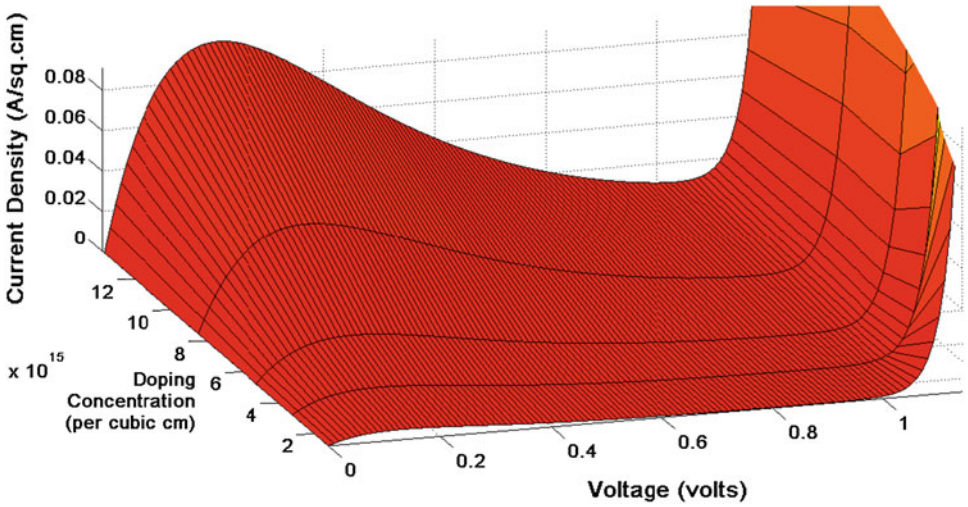

Fig. 6 Current density and voltage characteristics of GaAs tunneling layer for different doping concentrations

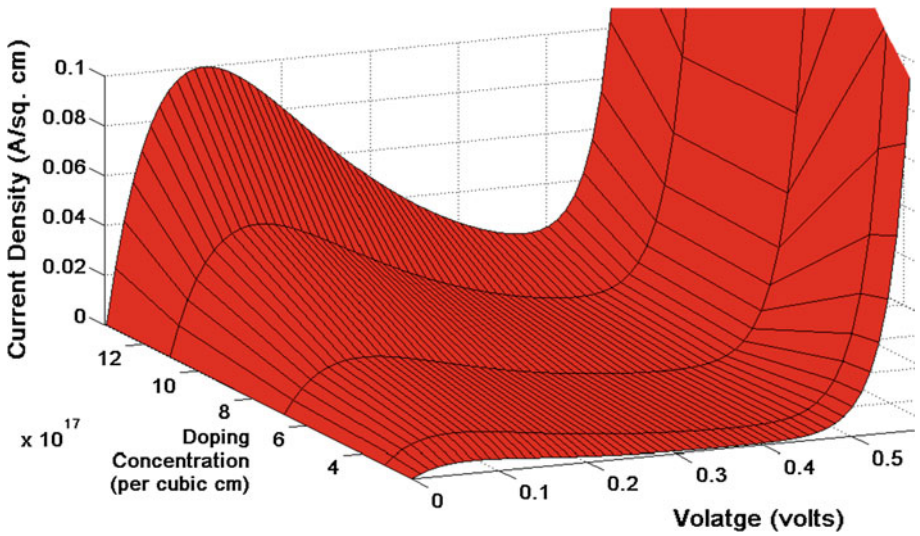

Fig. 7 Current density and voltage characteristics of Ge tunneling layer for different doping concentrations

Table 2 for GaAs. Figure 7 shows the current density versus voltage curves for different values of doping concentration for Ge tunneling layer. It can be observed from the simulation results that by increasing the doping concentration, the peak current density and voltage are increased. Moreover, it can also be observed that the ratio of the peak current density and valley current density is $\frac{1}{12}$ for GaAs and $\frac{1}{6}$ for Ge. It is also evident from the simulation results that the peak current density of the tunneling layer is same for peak voltage and forward voltage. It means that simulations produced by the model are in good agreement with realistic behavior of the tunneling layer.

A GaInP/GaAs/Ge triple-junction solar cell with GaAs tunneling junction and a GaInP/GaAs dual-junction solar cell (DJSC) with GaInP tunneling junction are considered for the simulation of MJSC model. The model assumes that all series resistances are small enough, such that hysteresis behavior will not be observed in the characteristics of the structure with solar cell and tunnel diode. Secondly, the simulations are performed at constant temperature of 300 K, and the effect of temperature changes is not modeled. By including these parameters, this model could represent a more detailed representation of MJSC.

Table 3 Open-circuit voltage, short-circuit current and energy bandgap of individual and integrated cells [31,32]

	V_{OC} (volts)	I_{SC} (mA/cm^2)	Eg (eV)
GaInP cell	1.3	11	1.9
GaAs cell	1.424	25.2	0.93
Ge cell	0.245	45.6	0.66
Triple-junction cell	2.651	17.73	3.91
Dual-junction cell	2.48	19	2.8

Table 3 shows that combination of GaInP, GaAs and Ge solar cells in multi-junction cell via window layer and tunnel layer results in higher open-circuit voltages than their individual respective cells. However, it is observed that because

Table 4 Major parameters for GaInP, GaAs and Ge [31,32]

	Lattice constant (A^0)	Permittivity (e_s/e_0)	Affinity (eV)	Heavy e^- effective mass (m_e^*/m_0)	Heavy h^+ effective mass (m_h^*/m_0)	e^- mobility ($cm^2/V.s$)	h^+ mobility ($cm^2/V.s$)	e^- density of states NC ($/cm^3$)	h^+ density of states NV ($/cm^3$)
Ge	5.66	16	4	1.57	0.28	3,900	1,800	1.04E+19	6.00E+18
GaAs	5.56	13.1	4.07	0.063	0.5	8,800	400	4.70E+17	7.00E+18
GaInP	5.65	11.6	4.16	3	0.64	1,945	141	1.30E+20	1.28E+19

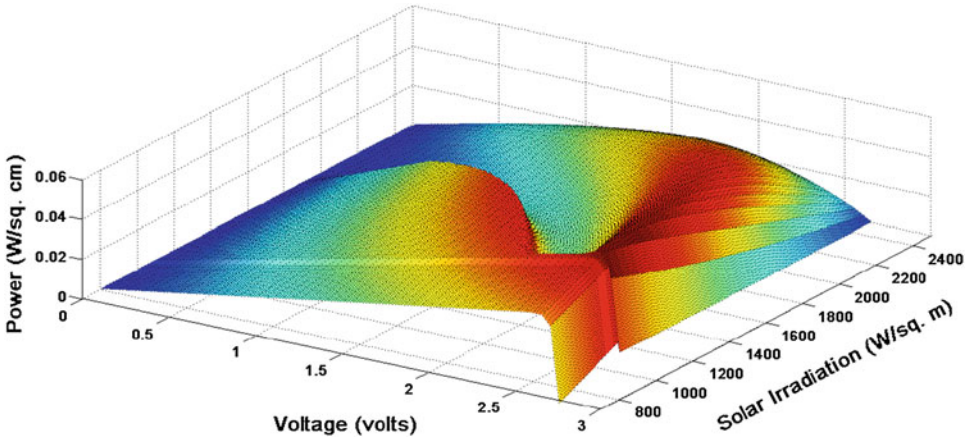

Fig. 8 Power and applied voltage characteristic curve for varying irradiation of triple-junction solar cell (InGaP/GaAs/Ge)

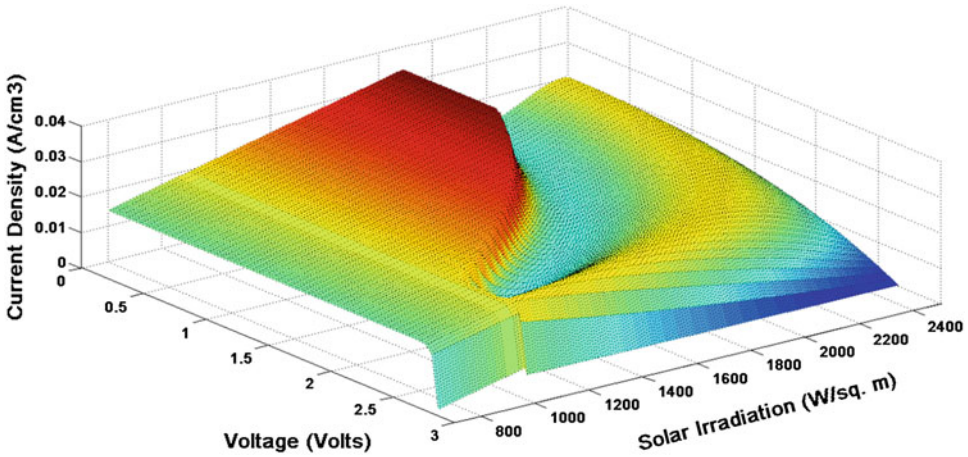

Fig. 9 Current density and applied voltage characteristic curve for varying irradiation of triple-junction solar cell (InGaP/GaAs/Ge)

of series-current matching, the collective cell current has been reduced to 17.73 mA/cm^2 with $V_{OC} = 2.651$ V. Similarly, the second cell structure produces $V_{OC} = 2.48$ V and $I_{SC} = 19$mA/cm^2. The parametric values of GaAs/GaAs and GaInP/GaInP tunnel junctions are given in Table 4.

It is evident from Eq. 2 that current density of solar cell is proportional to its photogenerated current, which has direct relation with solar irradiation. However, the voltage has a logarithmic relationship with the photogenerated current. Thus, increase in solar irradiation increases current density of the MJSC. If the current density of MJSC is smaller than the peak current density J_p of tunneling layer, then MJSC exhibits conventional solar cell behavior. However, when current density of device increases above J_p, then MJSC exhibits a change in P–V characteristics (Figs. 8 and 10). Figures 9 and 11 show applied voltage versus current density curve for different values of solar irradiation. In Fig. 9, tunneling layer of triple-junction solar cell (TJSC) results in dip as current density increases. This dip appears because of the negative resistance region in I–V characteristic of GaAs as shown in Fig. 2. However, dip does not appears in I–V curve of DJSC because GaInP does not have negative resistance region. The dip caused by GaAs junction keeps on increasing due to two major reasons; firstly, the valley current of the tunnel junction depends on the peak current of the tunnel junction. Moreover, the peak occurring during the backward sweep also corresponds to J_{peak}, but may be lower. Secondly, the potentials across the tunnel also alter which affects the

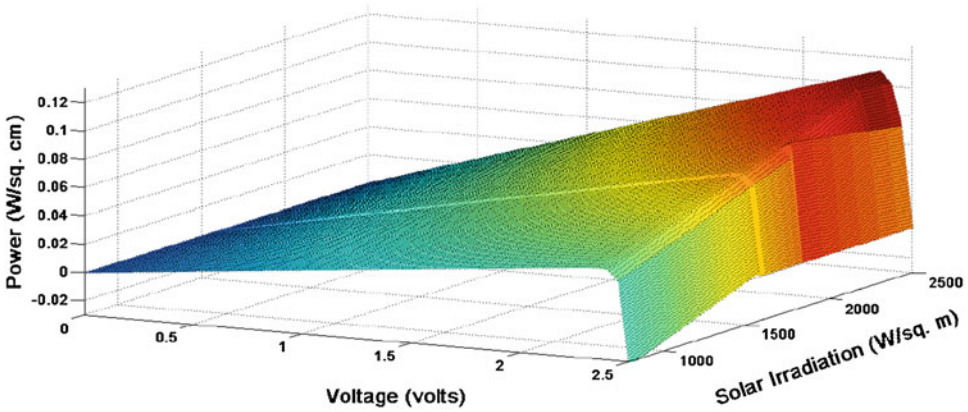

Fig. 10 Power and applied voltage characteristic curve for varying irradiation of double-junction solar cell (InGaP/GaAs)

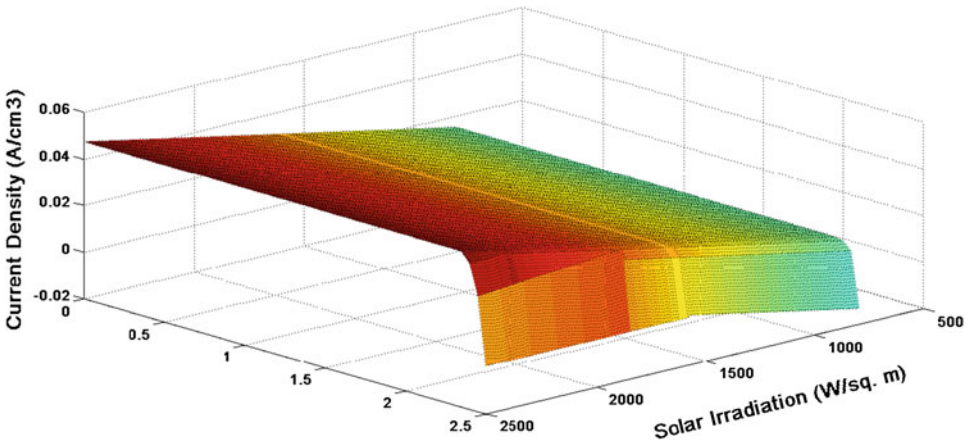

Fig. 11 Current density and applied voltage characteristic curve for varying irradiation of double-junction solar cell (InGaP/GaAs)

internal negative differential resistance of tunnel and thus modifies the valley voltage [10]. It is also evident from Fig. 9 that after the current density of solar cell becomes greater than the tunnel peak current density, the peak power of the system is disturbed. Moreover, power curve of TJSC exhibits two different peaks which make it impossible for system to track maximum power point. On the other hand, power of DJSC is reduced which is undesirable.

The simulation results show that for lower levels of concentration, the TJSC with GaAs tunnel junction would be a better choice. Upon increase in the level of solar insolation, this tunnel junction provides negative resistive path to the carries, instead of facilitating MJSC with negligible resistance path by tunnel layer. This could be managed by increasing the peak tunneling current of the GaAs junction. However, this problem would remain there since whenever the total cell current crosses the peak tunneling current, there would be dramatic change in its performance. This alteration in cell performance either has to be compensated by the power system or the cell should only be deployed to the area which has insolation level compatible with its operating range. This could be one of the trades-off for TJSC.

On the other hand, DJSC with GaInP is quite effective because it does not face such a drastic change in performance at different levels of insolation. However, it also alters the projected curve of the PV cell. But DJSC has lower optical absorption capability as compare to TJSC. DJSC can absorb maximum wavelength of 0.9 μm whereas TJSC can absorb maximum wavelength of 1.8 μm. It means DJSC does not utilize the photons which have wavelength greater than 0.9 μm. However, TJSC can utilize two times more energy-carrying photons compared with DJSC. This is trade-off of DJSC.

8 Conclusion

This paper covers a general mathematical model of MJSCs for simulating its characterization curves including current density and power curves as a function of voltage. The mathematical model of a tunneling layer is integrated to examine the effect of tunneling on I–V Characteristics of MJSC. Doping levels of realistic values have been presented to describe the slope of tunneling current for low voltages.

The model was tested by simulating two different MJSCs, i.e., InGaP–GaAs DJSC and InGaP–GaAs–Ge TJSC. The simulation results show realistic performance of tunneling junction at different levels of concentration for increasing applied voltage. Thus, it is inferred that I–V characteristics of

MJSC are sensitive to insolation because of tunnel layer. The simulation results are in full agreement with the experimental outcomes presented in literature which proves the efficacy and applicability of the model. The model is suitable for power and control system analysis of CPV systems and to identify the operation range of different MJSCs and develop possible control strategies to avoid undesirable situation.

References

1. Green, M.: Photovoltaic principles.Phys. E Low Dimens. Syst. Nanostructures **14**(1), 11–17 (2002)
2. Yamaguchi, M.; Takamoto, T.; Araki, K.; Ekins-Daukes, N.: Multi-junction iii–v solar cells: current status and future potential. Solar Energy **79**(1), 78–85 (2005)
3. Yamaguchi, M.: Super-high-efficiency mjscs. Prog. Photovolt. Res. Appl. **13**, 125 (2005)
4. Dimroth, F.; Kurtz, S.: High-efficiency multijunction solar cells. MRS Bull. **32**(03), 230–235 (2007)
5. Burnett, B.: The basic physics and design of iii–v multijunction solar cells. National Renewable Energy Laboratory, http://www.nrel.gov/ncpv/pdfs/11_20_dga_basics_9-13.pdf, summer (2002)
6. Martí, A.; Luque, A.: Next Generation Photovoltaics: High Efficiency Through Full Spectrum Utilization. Taylor & Francis, London (2004)
7. Sherif, R.; et al.: Concentrator triple-junction solar cells and receivers in point focus and dense array modules. Proceedings 21nd EU PVSEC-2006 (2006)
8. King, R.; Karam, N.; Ermer, J.; Haddad, N.; Colter, P.; Isshiki, T.; Yoon, H.; Cotal, H.; Joslin, D.; Krut, D.; et al.: Next-generation, high-efficiency iii-v multijunction solar cells. In: Photovoltaic Specialists Conference, 2000. Conference Record of the Twenty-Eighth IEEE, pp. 998–1001. IEEE (2000)
9. González, M.; Chan, N.; Ekins-Daukes, N.; Adams, J.; Stavrinou, P.; Vurgaftman, I.; Meyer, J.; Abell, J.; Walters, R.; Cress, C.; et al.: Modeling and analysis of multijunction solar cells. In: Proceedings of SPIE, vol. 7933, p. 79330R (2011)
10. Guter, W.; Bett, A.: I-v characterization of devices consisting of solar cells and tunnel diodes. In: Conference Record of the 2006 IEEE 4th World Conference on Photovoltaic Energy Conversion, vol. 1, pp. 749–752. IEEE (2006)
11. King, R.; Law, D.; Edmondson, K.; Fetzer, C.; Kinsey, G.; Yoon, H.; Sherif, R.; Karam, N.: 40percent efficient metamorphic gainp/gainas/ge multijunction solar cells. Appl. Phys. Lett. **90**(18), 183516 (2007)
12. Guter, W.; Schöne, J.; Philipps, S.; Steiner, M.; Siefer, G.; Wekkeli, A.; Welser, E.; Oliva, E.; Bett, A.; Dimroth, F.: Current-matched triple-junction solar cell reaching 41.1% conversion efficiency under concentrated sunlight. Appl. Phys. Lett. **94**, 223,504 (2009)
13. Spectrolab solar cell breaks 40percent efficiency barrier (2006). http://www.renewableenergyworld.com/rea/news/article/2006/12/solar-cell-breaks-the-40-efficiency-barrier-46765
14. Solar junction achieves world record solar cell conversion efficiency of 44percent (2011). http://www.solarserver.com/solar-magazine/solar-news/current/2012/kw42/solar-junction-achieves-world-record-solar-cell-conversion-efficiency-of-44.html
15. Esaki, L.: New phenomenon in narrow germanium pn junctions. Phys. Rev. **109**(2), 603 (1958)
16. Nikhil M, K.; Stephen, B.; Jennifer, H.; Michael, B.S.: Modelling of an esaki tunnel diode in a circuit simulator. Act. Passiv. Electron. Compon. **2011** (2011). http://dx.doi.org/10.1155/2011/830182
17. King, R.; Fetzer, C.; Colter, P.; Edmondson, K.; Ermer, J.; Cotal, H.; Yoon, H.; Stavrides, A.; Kinsey, G.; Krut, D.; et al.: High-efficiency space and terrestrial multijunction solar cells through bandgap control in cell structures. In: Conference Record of the 29th IEEE Photovoltaic Specialists Conference, 2002.; pp. 776–781. IEEE (2002)
18. W. Guter F. Dimroth, M.M.; Bett, A.W.: Tunnel diodes for iiiv multi-junction solar cells. Photovoltaic Solar Energy Conf.; Barcelona, Spain p. 515–518 (2005)
19. Guter, W.; Bett, A.: I–v characterization of tunnel diodes and multijunction solar cells. IEEE Trans. Elect. Dev. **53**(9), 2216–2222 (2006)
20. Hermle, M.; Letay, G.; Philipps, S.; Bett, A.: Numerical simulation of tunnel diodes for multi-junction solar cells. Prog. Photovolt. Res. Appl. **16**(5), 409–418 (2008)
21. Jung, D.; Parker, C.; Ramdani, J.; Bedair, S.: Algaas/gainp heterojunction tunnel diode for cascade solar cell application. J. Appl. Phys. **74**(3), 2090–2093 (1993)
22. Takamoto, T.; Ikeda, E.; Kurita, H.; Ohmori, M.: Over 30percent efficient ingap-gaas tandem solar cells. Appl. Phys. Lett. **70**, 381 (1997)
23. Ahmed, S.; Melloch, M.; Harmon, E.; McInturff, D.; Woodall, J.: Use of nonstoichiometry to form gaas tunnel junctions. Appl. Phys. Lett. **71**, 3667 (1997)
24. Chiang, P.; Timmons, M.; Hutchby, J.: Patterned germanium tunnel junctions for multijunction monolithic cascade solar cells. Solar Cells **21**(1–4), 241–252 (1987)
25. Gibson, G.; Meservey, R.: Properties of amorphous germanium tunnel barriers. J. Appl. Phys. **58**(4), 1584–1596 (1985)
26. Gow, J.; Manning, C.: Development of a photovoltaic array model for use in power-electronics simulation studies. In: IEEE Proceedings—Electric Power Applications, vol. 146, pp. 193–200. IET (1999)
27. Wasynezuk, O.: Dynamic behavior of a class of photovoltaic power systems. IEEE Trans. Power Apparatus Syst. **9**, 3031–3037 (1983)
28. Phang, J.; Chan, D.; Phillips, J.: Accurate analytical method for the extraction of solar cell model parameters. Electron. Lett. **20**(10), 406–408 (1984)
29. Tsai, H.; Tu, C.; Su, Y.: Development of generalized photovoltaic model using matlab/simulink. In: Proceedings of the World Congress on Engineering and Computer Science, pp. 846–851. Citeseer (2008)
30. Bube, R.; Bube, R.: Photovoltaic Materials, vol. 1. Imperial College Press, London (1998)
31. Streetman, B.; Banerjee, S.: Solid State Electronic Devices, vol. 2. Prentice-Hall, New Jersey (1995)
32. Bube, R.; Bube, R.: Photovoltaic Materials, vol. 1. Imperial College Press, London (1998)
33. Sagol, B.; Szabo, N.; Doscher, H.; Seidel, U.; Hohn, C.; Schwarzburg, K.; Hannappel, T.: Lifetime and performance of ingaasp and ingaas absorbers for low bandgap tandem solar cells. In: 34th IEEE Photovoltaic Specialists Conference (PVSC), 2009, pp. 001090–001093. IEEE (2009)
34. Sterzer, F.: Stability of tunnel-diode osciallators. In: 16th Annual Symposium on Frequency Control, pp. 391–404. IEEE (1962)
35. Oscillator diode gallium arsenide. http://www.datasheetarchive.com/Custom+Components-datasheet.html
36. Oscillator diode germanium. http://www.datasheetarchive.com/Custom+Components-datasheet.html